MOLECULAR AND CELLULAR BIOLOGY, Nov. 1995, p. 6341–6350 Vol. 15, No. 11
0270-7306/95/$04.00+0

The Amino-Terminal Domain of Yeast U1-70K Is Necessary and Sufficient for Function

PATRICIA J. HILLEREN, HUNG-YING KAO, AND PAUL G. SILICIANO*

Department of Biochemistry and Institute of Human Genetics, University of Minnesota, Minneapolis, Minnesota 55455

Received 10 July 1995/Returned for modification 8 August 1995/Accepted 25 August 1995

The *Saccharomyces cerevisiae SNP1* gene encodes a protein that shares 30% amino acid identity with the mammalian U1 small nuclear ribonucleoprotein particle protein 70K (U1-70K). We have demonstrated that yeast strains in which the *SNP1* gene was disrupted are viable but exhibit greatly increased doubling times and severe temperature sensitivity. Furthermore, *snp1*-null strains are defective in pre-mRNA splicing. We have tested deletion alleles of *SNP1* for their ability to complement these phenotypes. We found that the highly conserved RNA recognition motif consensus domain of Snp1 is not required for complementation of the *snp1*-null growth or splicing defects nor for the in vivo association with the U1 small nuclear ribonucleoprotein particle. However, the amino-terminal domain of Snp1, less strongly conserved, is necessary and sufficient for complementation.

Pre-mRNA splicing requires the action of the U1, U2, U4/U6, and U5 small nuclear ribonucleoprotein particles (snRNPs). The snRNPs function in splicing by associating with one another and with conserved sequences in the intron (9, 41). snRNPs are stable, abundant, and highly conserved particles consisting of small nuclear RNA molecules (snRNAs) complexed with sets of proteins (30). While many functionally important interactions involving the RNA components of the snRNPs have been described (21, 27, 31, 38, 40, 48, 60, 63), the functions of the snRNP proteins in splicing are largely unknown.

During splicing, the U1 snRNP interacts with the 5′ splice site of the pre-mRNA and interacts as well with the branch site region (46, 51) and (in some cases) the 3′ splice site (44). Interaction with the 5′ splice site requires both the 5′ end of the U1 RNA and the protein components of the snRNP (8, 35). This interaction takes place at least in part by RNA-RNA base pairing (50, 53, 63), but the ways in which the U1 snRNP proteins contribute to this interaction have not been elucidated.

Metazoan U1 snRNP contains the 164-nucleotide U1 snRNA, which adopts a conserved secondary structure consisting of three internal stem-loop structures (36). At least eleven proteins are stably complexed with the U1 RNA, including the group of Sm proteins (B, B′, D1, D2, D3, E, F, and G) that are common to all splicing snRNPs (4, 6, 18, 26). These proteins bind to the conserved sequence $AU_{4-6}G$ in snRNAs and are thought to be required for snRNP stability (20) and nuclear localization (33).

The U1 snRNP also contains three U1-specific proteins called A, C, and 70K (30). The 70K protein binds directly to stem-loop I of U1 snRNA (17, 42, 57), while the A protein binds directly to stem-loop II. Protein C is thought to interact with stem-loop I (17), but it is not known if this interaction is direct. Interestingly, protein C was shown in vitro to require the U1-70K protein to assemble with the human U1 snRNP (37). Biochemically fractionated core U1 snRNPs contain the full complement of Sm proteins but are stripped of the U1 snRNP-specific proteins 70K, A, and C (3). Using in vitro-translated proteins, it was shown that the U1-C protein is unable to independently associate with core U1 snRNPs, requiring the 70K protein but not protein A (37).

Among metazoans, 70K is highly conserved (88% amino acid identity between human 70K and *Xenopus laevis* 70K [13, 32]) and contains an RNA recognition motif (RRM) consensus domain, a sequence feature common to many RNA-binding proteins (2, 12). In addition to the RRM domain, metazoan 70K contains a glycine-rich region downstream of the RRM domain. The glycine-rich region contains several RGG-like repeats implicated in RNA binding (11) and may act as an auxiliary domain for specific RNA binding. The carboxyl tail of human U1-70K is rich in arginine. An RS domain characterized by several arginine-serine dipeptides is embedded within this region. The RS domain is a hallmark of a family of splicing factors, including SF2/ASF and $U2AF^{65}$, that are required for in vitro splicing (5, 7, 62). The serine residues of the human U1-70K RS domain are phosphorylated in vitro by a U1 snRNP-associated kinase activity (61). Furthermore, the phosphorylation state of the human U1-70K critically affects a precatalytic step of in vitro splicing reactions (59).

The association of human U1-70K within the U1 snRNP is bipartite (37). Studies of human U1-70K have defined the minimal U1 RNA binding domain to be a 110-amino-acid region containing the RRM domain plus flanking amino acids including most of the glycine-rich domain (42, 57). This region is necessary and sufficient to bind the 70K protein to U1 RNA. However, the amino-terminal region (amino acids [aa] 1 to 97) of human U1-70K lacking the RRM domain efficiently associates with core U1 snRNPs (37). The association of the amino-terminal U1-70K fragment with the core U1 snRNP is presumably dependent on one or more Sm proteins, as it fails to bind naked U1 RNA (37).

Saccharomyces cerevisiae U1 RNA is homologous to metazoan U1 and is required for viability (25, 54). The stem-loop I structure of yeast U1 RNA is similar to that of human U1 RNA, including precise conservation of 9 of 10 nucleotides in loop I. However, mutagenesis of stem-loop I of yeast U1 RNA yielded the surprising result that severe mutations in stem-loop I are viable, although they did cause a moderate reduction in splicing efficiency (28). These results suggested that the yeast

* Corresponding author. Mailing address: Department of Biochemistry, University of Minnesota, 4-225 Millard Hall, 445 Delaware St. SE, Minneapolis, MN 55455. Phone: (612) 625-4928. Fax: (612) 625-2163. Electronic mail address: pauls@lenti.med.umn.edu.

TABLE 1. Yeast strains used

Strain	Genotype	Source
YPH400	*MAT***a**/*MAT*α *ade2-101*/*ade2-101 his3-Δ200*/*his3-Δ200 leu2-Δ1*/*leu2-Δ1 lys2-801*/*lys2-801 trp1-Δ63*/*trp1-Δ63 ura3-53*/*ura3-53*	J. Milligan
YPH401	Same as YPH400 except *SNP1*/*snp1*::*ADE2*	This work
2A	*MAT***a** *SNP1* segregant of YPH401	This work
2B	*MAT*α *SNP1* segregant of YPH401	This work
2C	*MAT*α *snp1*::*ADE2* segregant of YPH401	This work
2D	*MAT***a** *snp1*::*ADE2* segregant of YPH401	This work
a/α100	*MAT***a**/*MAT*α *ade2-1*/*ade2-1 can1-100*/*can1-100 his3*/*HIS3 his4*/*HIS4 leu2*/*leu2 trp1*/*trp1 ura3*/*ura3*	V. Smith
a/α105	*MAT***a**/*MAT*α *ade2-1*/*ade2-1 can1-100*/*can1-100 leu2*/*leu2 trp1*/*trp1 ura3*/*ura3 his3*/*HIS3 his4*/*HIS4 SNP1*/*snp1*::*ADE2*	This work
105-2A	*MAT***a** *snp1*::*ADE2* segregant of **a**/α105	This work

U1 snRNP does not require 70K function or that yeast 70K could remain associated with the U1 snRNP without binding to stem-loop I, presumably by interacting with other parts of the U1 snRNA or with other U1 snRNP proteins.

The yeast *SNP1* gene encodes the Snp1 protein, which has 30% overall amino acid identity to human 70K (56). The RRM and glycine-rich domains are well conserved from yeasts to humans, but the arginine-rich carboxyl terminus is not evident in *SNP1*. Gene disruption experiments showed that *SNP1* encodes a protein essential for yeast viability (56). We have previously shown that Snp1 binds specifically and directly to stem-loop I of yeast U1 RNA (22). In addition, coimmunoprecipitation experiments showed that Snp1 is a stable component of the U1 snRNP (1).

To determine the function of the 70K protein in splicing, we initiated a genetic analysis of the *SNP1* gene in yeast cells. In contrast to the findings of Smith and Barrell (56), we found that yeast cells are viable in the absence of an intact *SNP1* gene. However, *snp1*-null cells exhibit a pre-mRNA splicing defect and dramatically increased doubling times. To map the functional domains of the Snp1 protein, we made a series of deletions that removed regions within the amino terminus and the RRM, glycine-rich (Gly), and carboxyl-terminal domains. *snp1* alleles that lack the RRM, glycine-rich, and carboxyl-terminal domains are able to complement the severe phenotypes of *snp1*-null cells. In strong contrast, deletions in the amino-terminal domain abolished complementation activity. We show that the amino terminus is necessary for complementation of the splicing defect, the growth defect, and snRNP association. Thus, the functional regions of Snp1 are mapped to the amino-terminal domain.

MATERIALS AND METHODS

Construction of the snp1 disruption allele. The plasmid pD1 containing the *SNP1* gene was a gift of V. Smith. A 2,394-bp *Spe*I-*Dra*I fragment that contains the entire coding region of *SNP1* plus 707 nucleotides upstream and 787 nucleotides downstream was subcloned into Bluescript KS at the *Spe*I and *Sma*I restriction sites, creating the plasmid BS-*SNP1*. The *snp1*::*ADE2* disruption allele deletes more than 90% of the coding region and replaces it with the *ADE2* gene. The allele was constructed by subcloning the desired fragments into Bluescript KS + (Stratagene) in three phases as follows. First, an *Afl*III-*Xba*I fragment of BS-*SNP1* encompassing 701 nucleotides of 5′ untranslated sequence and 35 nucleotides of the *SNP1* amino-terminal coding region was subcloned into Bluescript KS at the *Spe*I-*Xba*I restriction sites, creating the phase I disruption construct. Second, an *Xho*I-PstI *SNP1* fragment from BS-*SNP1* encompassing 41 nucleotides of the carboxyl-terminal coding region and 787 bp of 3′ untranslated sequence was subcloned into the *Sma*I-*Pst*I restriction sites of the phase I disruption construct, creating the phase II disruption construct. A single *Bam*HI restriction site separates the two subcloned *SNP1* fragments in the phase II construct. A 3.6-kb *Bam*HI fragment encoding the *ADE2* gene was subsequently subcloned into the *Bam*HI site in the phase II construct, generating the *snp1*::*ADE2* disruption allele. This allele deletes all but 11 amino-terminal and 13 carboxyl-terminal aa of the *SNP1* coding region. For integrative transformation into yeast cells, the disruption allele was cut out with *Pst*I and *Sst*I.

Yeast methods. The yeast strains used in this study are described in Table 1. YPH400 was derived from YPH399 (P. Hieter) by J. Milligan, and **a**/α100 and **a**/α115 were provided by V. Smith. Standard yeast media were used (52). Yeast transformations were performed by the method of Ito et al. (19). Integration of the disruption allele was complicated by the ability of the disruption allele fragment to be maintained extrachromosomally. We believe this is due to the presence of an ARS sequence in the *SNP1* flanking regions. To identify cells in which the disruption allele fragment had integrated, stable adenine prototrophs were selected after extended growth in yeast extract-peptone-dextrose medium. Dissection plates were incubated at 23°C in a humidified chamber, and colony formation was observed for a period of at least 2 weeks.

Southern analysis. Genomic DNA (2 μg) was digested with *Spe*I (Boehringer Mannheim Biochemicals) and electrophoresed through a 0.8% agarose gel. Direct gel hybridization (Clontech protocol) was carried out by using [α-^{32}P]dCTP-labeled ([α-^{32}P]dCTP from Amersham) *Eco*RV-*Sst*I fragments of *SNP1* from BS-*SNP1*. The probe was synthesized to a specific activity of 10^9 cpm/μg by using a random hexamer priming kit (Pharmacia).

RNA analysis. Total RNA was prepared according to the method of Domdey et al. (10). Primer extension was performed according to the method of Frank and Guthrie (15). For each sample, 25 μg of total RNA was incubated with 10^6 cpm of ^{32}P-labeled oligonucleotide. Oligonucleotides specific to the transcripts analyzed are as follows: *MAT***a**1, 5′-GAATTTATTTAGATCTCATACGTTT-3′; *U3A*/*U3B*, 5′-CCAAGTTGGATTCAGT-3′; *SAR1*, 5′-TACCATGTTTGTTC CACAGA-3′; *U6*, 5′-TGCTGATCATCTCTGTATTG-3′; and *U5*, 5′-AAGCG CATAGTAAGAC-3′. For Northern (RNA) blot analysis of snRNAs, the following oligonucleotides were end labeled by T4 polynucleotide kinase and [γ-^{32}P]ATP: *U2*, 5′-AAGAACAGATACTACACTTG-3′; *U1*, 5′-GTTACT GAAGTTACTTGTTAATA-3′; and *U5*, 5′-AAGCGCATAGTAAGAC-3′.

Splicing extracts. Splicing extracts were prepared according to the method of Lin et al. (29).

Preparation of antisera to the TrpE-Snp1 fusion protein. The TrpE-Snp1 fusion protein was overexpressed as described previously (22). To gel purify the fusion protein, the pellet fraction was resuspended in sodium dodecyl sulfate (SDS)-polyacrylamide gel electrophoresis sample buffer and the proteins were separated on preparative SDS-7% polyacrylamide gels. The TrpE-Snp1 fusion protein was excised from the gels and electroeluted in 0.05 M NH_4HCO_3–0.1% (wt/vol) SDS (55). The samples were dialyzed against 1× phosphate-buffered saline (PBS) and concentrated by Centriprep (Amicon). Three rabbits were injected with 500 μg of gel-purified TrpE-Snp1 and given a booster shot of 250 μg every 4 weeks by the Berkeley Antibody Company. The rabbit sera were affinity purified by passage over a TrpE-Snp1 fusion protein-coupled Affi-Gel 10 column (BioRad). Affinity-selected antisera were eluted with 2 M glycine-HCl, pH 2.5, and then dialyzed against 1× PBS containing 0.02% sodium azide.

Allele construction. Transformer mutagenesis (Clontech kit 1600-1) was used to engineer blunt-end restriction sites and point mutations into BS-*SNP1*. Oligonucleotide N-1, 5′-GACTTTTCAAGCCCGGGCCACC-3′, generated a *Sma*I site between aa 18 and 19, converting aa 19 from arginine to glycine. Oligonucleotide N-3, 5′-GACATCAAACTTTCGCGAATCAAAAATGCTC-3′, generated an *Nru*I site between aa 77 and 78, converting aa 78 from lysine to arginine. Oligonucleotide N-4, 5′-CCGGAGACTACAAAATGTTAACCCTAACG-3′, generated an *Hpa*I site between aa 92 and 93, converting aa 92 from tryptophan to valine. Combinatorial subcloning utilizing the engineered, blunt-end restriction sites and an endogenous blunt-end *Eco*47III restriction site (aa 247 and 248) yielded the alleles Δ59, Δ74, Δ16, Δ156, and Δ169. The carboxyl-terminal truncation allele was engineered by utilizing oligonucleotide C-1, 5′-GGAAG GTTTTGAAGCGCAAG-3′, which generated a premature stop codon at amino acid 220. The mutant Oct allele converted three residues within RNP1 as follows: a K-to-L mutation at position 148 (K148L), Y150T, and F152L. This allele was generated by utilizing oligonucleotide mOct, 5′-GAAGAGTCTAGGCACCGC CTTGATAGTTTTC-3′, in transformer mutagenesis. The ΔGly allele was gen-

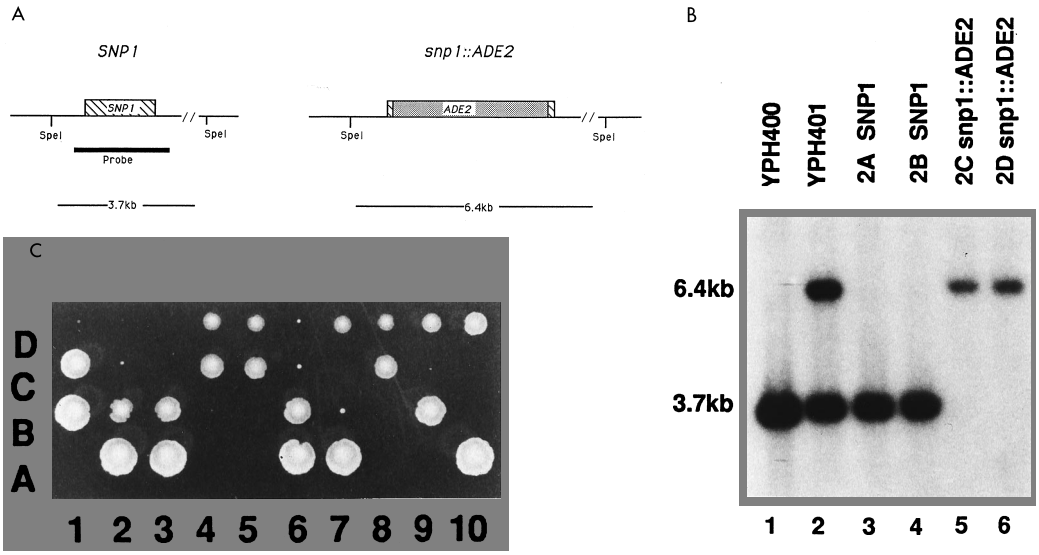

FIG. 1. Disruption of the *SNP1* locus. (A) The genomic *SNP1* locus and the *snp1*::*ADE2* disruption allele are depicted. Also shown are the expected sizes of *Spe*I fragments from both alleles and the probe used for Southern analysis in panel B. (B) Genomic DNAs of the wild-type strain YPH400, the *snp1*::*ADE2*/*SNP1* heterozygous diploid YPH401, and the four sister spores of tetrad 2 were digested with *Spe*I and analyzed by Southern blotting. The wild-type *SNP1* allele is contained on a 3.7-kb *Spe*I fragment, and the *snp1*::*ADE2* allele is contained on a 6.4-kb fragment. The blot shows the wild-type fragment of YPH400 (lane 1), one wild-type and one *snp1*::*ADE2* disruption allele of YPH401 (lane 2), wild-type *SNP1* in spores 2A and 2B (lanes 3 and 4), and the *snp1*::*ADE2* disruption allele in spores 2C and 2D (lanes 5 and 6). (C) Columns 1 to 10 are 10 individual tetrads with spores placed vertically at positions A to D. Three of these ten dissections yielded four-spored tetrads (2, 6, and 10), each with two fast-growing (*SNP1*) and two slowly growing (*snp1*::*ADE2*) spores. All available markers were tested and segregated independently. Wild-type spores at position D appear smaller than those at position A because of depletion of nutrients caused by growth of cells at the center of the plate (not shown). This difference disappears after isolation to fresh media.

erated by a PCR strategy. First, two PCR fragments that border the glycine-rich (Gly) domain deletion were generated. A 561-nucleotide amino-terminal fragment that contained an *Nhe*I site at the 3′ end just after aa 181 (PCR oligonucleotides 70K AUG, 5′-GCGGATCCATATGAATTATAATCTATCC-3′, and ΔGlyI, 5′-CGGGCTAGCGCAGATTCTGTCTTTCATTTGG-3′) was amplified. The 348-nucleotide carboxyl-terminal fragment that contained an *Nhe*I site at the 5′ end just prior to aa 208 (PCR oligonucleotides ΔGlyII, 5′-CGGG CTAGCTATTCCAACAGAGACAGCAGG-3′, and 70K F, 5′-TAACTGATGT GCGGGTAATC-3′) was amplified. The two PCR fragments were digested with *Nhe*I and subsequently ligated to yield an 899-nucleotide fragment carrying an in-frame deletion of 26 aa within the glycine-rich domain. The regeneration of the *Nhe*I restriction site codes for two novel amino acids, alanine and serine, at the deletion junction. This 899-nucleotide fragment was then digested with *Nde*I and *Xho*I to yield a 710-nucleotide fragment and was subcloned into BS-*SNP1* *Nde*I-*Xho*I. All BS-*snp1* mutant alleles were sequenced to confirm in-frame deletions and point mutations. Subsequently, they were subcloned into the centromere-based plasmid pRS315 and sequenced again to confirm allele identity.

Coimmunoprecipitation of Snp1 and U1 snRNA. Affinity-purified anti-TrpE-Snp1 antiserum (100 μl) was coupled with 40 μl of protein A-agarose (Sigma) in Ipp500 buffer (500 mM NaCl) for 1 h at 23°C (16). All reactions were performed in a final volume of 500 μl. Beads were washed three times in Ipp150 buffer (150 mM NaCl) and then incubated with 25 μl of yeast splicing extract in Ipp150 for 1 h at 23°C. After brief centrifugation, supernatants were removed and saved. Pellets were washed three times in Ipp150, with final suspension in 500 μl of Ipp150. RNA was recovered from the supernatants and pellets and was then analyzed for snRNAs by Northern blotting with γ-^{32}P-labeled probes. After autoradiography, the film was analyzed by densitometry to determine the efficiency of U1 RNA coimmunoprecipitation.

In vitro transcription. Plasmid pT719 was a kind gift from D. McPheeters. It contains the yeast U1 gene under the control of the T7 phage promoter. A *Bcl*I linearized template was used to in vitro transcribe a 47-nucleotide fragment encompassing stem-loop I of U1 RNA (U1/*Bcl*I) to a specific activity of ~1.1 × 10^7 cpm/μg with [α-^{32}P]UTP as previously described (22, 34).

Construction of *trpE-snp1* mutant alleles and fusion protein expression. Construction of the pATH3a-*trpE-SNP1* fusion allele was previously described (22). A PCR strategy was employed to amplify the entire coding region of each of the BS-*snp1* mutant alleles. The amplified products were then swapped into the corresponding region of pATH3a-*trpE-SNP1*. The oligonucleotides used in the PCRs were 70K AUG, 5′-GCGGATCCATATGAATTATAATCTATCC-3′, and 70K F, 5′-TAACTGATGTGCGGGTAATC-3′. The resulting PCR products were subsequently digested with *Bam*HI and *Xba*I and swapped into the vector backbone of a *Bam*HI-*Xba*I-digested pATH3a-*trpE-SNP1* construct. The *trpE*-Δ59, *trpE*-Δ74, *trpE*-mOct, *trpE*-ΔGly, *trpE*-mOct-ΔGly, *trpE*-Δ156, *trpE*-Δ169, and *trpE*-ΔC-1 constructs were each sequenced to confirm the in-frame fusion of the mutant *snp1* allele to *trpE* and the identity of deletion or mutant alleles. Overexpression of the TrpE-Snp1 mutant proteins was carried out as previously described (22, 23) with the bacterial strain CAG456.

Mobility shift assay. For each reaction, 0.5 to 1.0 pmol of in vitro-synthesized U1/*Bcl*I RNA (stem-loop I) was denatured at 70°C and slowly renatured in 1.5 mM $MgCl_2$. Approximately 5 μg of fractionated extract from each *trpE-snp1* mutant-transformed strain was incubated with denatured-renatured U1/*Bcl*I transcript for 30 min in 10 mM Tris (pH 8.0)–60 mM NaCl–10% glycerol–0.05% Nonidet P-40 in a 20-μl reaction mixture. Protein-RNA complexes were resolved by electrophoresis in a 5% acrylamide gel (acrylamide-bisacrylamide, 29.2:0.8) as previously described (22). The gels were dried and visualized by autoradiography.

RESULTS

***snp1*-null strains are viable.** The *snp1*::*ADE2* disruption allele (Fig. 1A) was used to disrupt a single copy of *SNP1* in the diploid strain YPH400, generating the *snp1*::*ADE2*/*SNP1* heterozygous diploid YPH401. Integration of a single copy of the *snp1*::*ADE2* disruption allele at the *SNP1* locus on one chromosome was confirmed by Southern analysis (Fig. 1B, lane 2).

Strain YPH401 was sporulated, and tetrads were dissected onto yeast extract-peptone-dextrose plates. Spores inheriting the wild-type *SNP1* gene formed visible colonies within 2 days at 23°C. In contrast, sister spores inheriting the *snp1*::*ADE2* allele formed visible colonies approximately 10 days after dissection (Fig. 1C). The Ade2$^+$ and slow colony formation phenotypes cosegregated. Southern analysis of the tetrads revealed the 2:2 segregation of the *SNP1* and the *snp1*::*ADE2* alleles (Fig. 1B, lanes 3 to 6). The presence of intact disruption alleles indicates that the viable spores did not result from loss of the disruption allele by gene conversion. In this dissection, 50% of the *snp1*-null spores yielded viable colonies. We believe that *snp1*-null spores are on the threshold of viability and that the low spore viability reflects their difficulty in getting through germination into vegetative growth. Interestingly, YPH401 tetrads dissected onto galactose medium resulted in approximately 90% *snp1*-null spore viability (data not shown). Thus, in

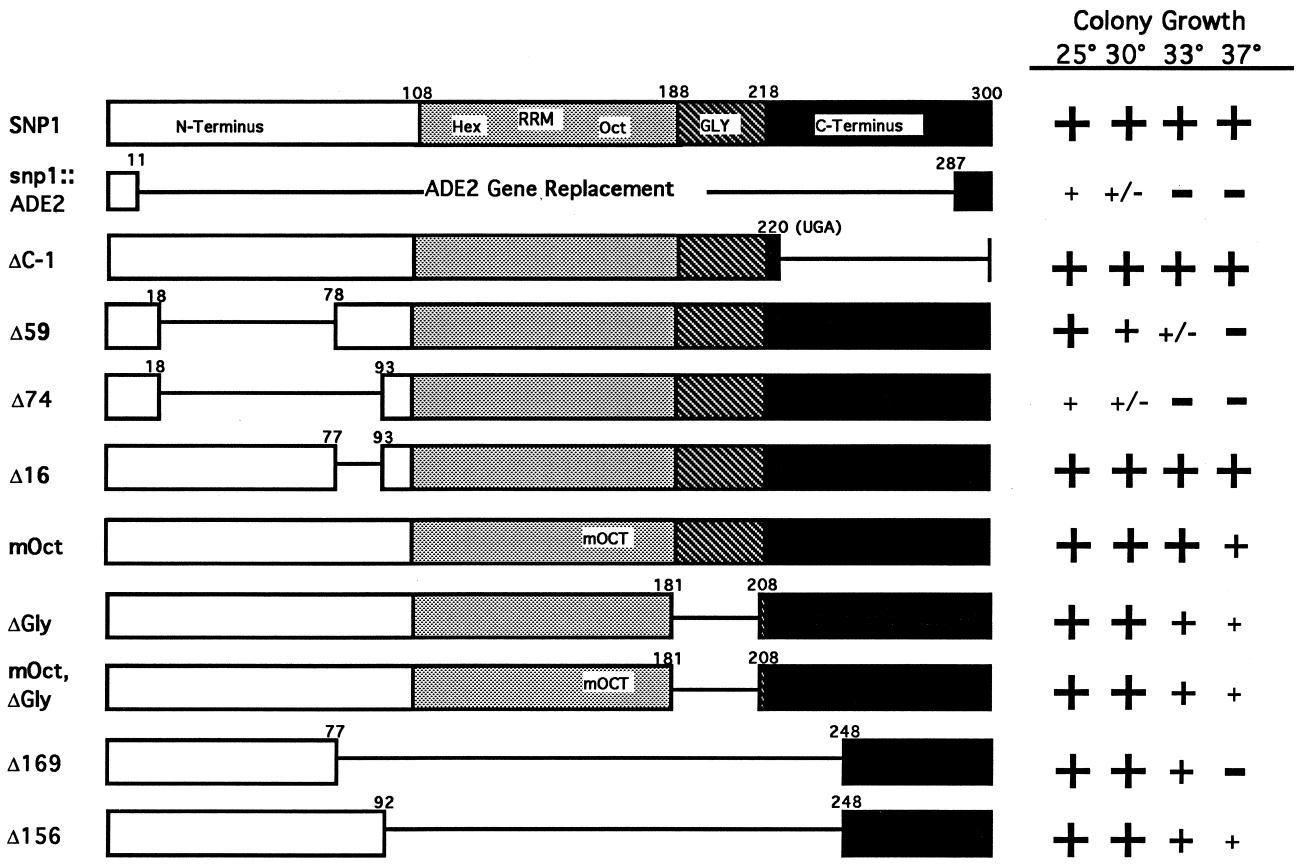

FIG. 2. *snp1* deletion alleles. Diagrammed are the domains of Snp1 and of the mutant Snp1 proteins. The borders of the RRM and glycine-rich domains were assigned on the basis of alignment to metazoan U1-70K. Thin lines represent the deleted regions of each protein, with the positions of the bordering amino acids indicated. The construction of each allele is described in Materials and Methods. The allele names correspond to the number of deleted amino acids within the indicated domains with the following exceptions: the ΔC-1 allele converted an alanine at position 220 to a UGA stop codon; the mOct allele converted three (in boldface type) of the eight highly conserved RNP1 amino acids (from **K**G**Y**A**F**IVF to **L**G**T**A**L**IVF); and the ΔGly allele removed 26 aa in the glycine-rich region but introduced two novel amino acids, alanine and serine, at the deletion junction. The ability to complement the *snp1*-null growth and temperature sensitivity phenotypes at various temperatures is indicated to the right of each mutant allele. The large, medium-sized, and small plus signs indicate wild-type, intermediate, and poor growth, respectively. The plus-minus combination indicates very poor growth, and the minus sign indicates failure to grow.

contrast to an earlier report (56), we found that yeast cells can be viable in the absence of an intact *SNP1* gene.

To reconcile these results, we obtained strain **a**/α100 from V. Smith and disrupted that strain with the *snp1*::*ADE2* allele to yield the heterozygous *SNP1*/*snp1*::*ADE2* diploid, **a**/α105. When dissected onto glucose medium, this strain does not give rise to viable *snp1*-null colonies. However, we were able to recover viable *snp1*-null strains when **a**/α105 was dissected on galactose medium. Once recovered from galactose medium, the **a**/α105-derived *snp1*-null strains are viable in glucose medium, with growth rates that parallel those of the YPH401-derived *snp1*-null strains. We believe that one difference in the viability of YPH401 and **a**/α105 *snp1*-null strains is due to the presence of a preexisting suppressor in the YPH401 genetic background and that the activity of this suppressor is carbon source dependent (17a).

Though viable, the *snp1*-null spores derived from both YPH401 and **a**/α105 strains grow very slowly in glucose medium. The doubling times of YPH401-derived *snp1*-null strains 2C and 2D are approximately fivefold longer than those of the wild-type sister strains 2A and 2B at 25°C (data not shown). This growth defect is not due to destabilization of U1 RNA, as *snp1*-null strains contain levels of U1 RNA similar to those of *SNP1* strains (see Fig. 6, lanes 1 and 4). The *snp1*-null strains are also strongly temperature sensitive, growing very slowly at 30°C and failing to grow at 33°C (see below).

Mapping the functional domains of *SNP1*. To characterize the functional domains of the yeast 70K protein, we constructed a set of deletion alleles that remove various regions of Snp1. The deletion alleles are diagrammed in Fig. 2. We first tested each deletion allele for the ability to complement the growth defect and the temperature sensitivity of *snp1*-null strains. We transformed the **a**/α105-derived *snp1*-null strain, 105-2A, with each of the mutant *snp1* alleles. The null strain was also transformed with the wild-type *SNP1* allele and, as a negative control, was transformed with the pRS315 vector alone. Transformation with the wild-type *SNP1* allele provides wild-type growth, whereas the pRS315 vector-transformed strain displays the null phenotype: slow growth at 25°C, extremely slow growth at 30°C, and no growth at 33°C (Fig. 3).

The slow growth and temperature sensitivity defects are complemented by many *snp1* deletion alleles (Fig. 3). For example, ΔC-1, which lacks the C-terminal 80 aa, restores wild-type growth to the *snp1*-null strain. Deletions in the amino-terminal domain, however, result in stronger phenotypes. The Δ59 allele removes 59 aa within the amino terminus and complements the growth defect of the *snp1*-null strain at 25 and 30°C but allows only poor growth at 33°C. A larger dele-

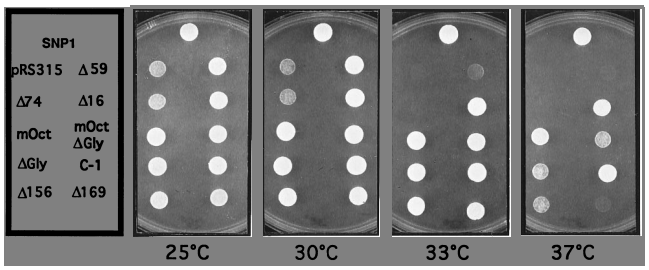

FIG. 3. Growth of *snp1* mutants. The *snp1*-null strain 105-2A was transformed with each mutant *snp1* allele as well as the wild-type *SNP1* allele and the pRS315 vector containing no *SNP1* insert. Single transformants were colony purified and subsequently assayed for their corresponding growth phenotypes at various temperatures. Shown are the results of growth of each of the wild-type *SNP1*, mutant *snp1*, and *snp1*-null (pRS315) strains. Approximately 15,000 cells from each strain were spotted onto selective media and incubated at the indicated temperature for 48 h. The key on the left indicates the arrangement of strains on the plants.

tion in the amino terminus, Δ74, displays a growth pattern identical to that of the null strain, indicating that this allele fails to complement at all. These results indicated that the amino-terminal domain contains residues important for Snp1 function and suggested that a region of the amino-terminal domain retained in Δ59 but removed in Δ74 was especially critical for Snp1 activity. To test this proposal, we constructed Δ16, which deletes only this overlap region. However, Δ16 complements fully, suggesting that redundant functional domains exist in the Snp1 protein and that Δ74 disrupts both of these functional domains. Alternatively, the Δ74 allele may have failed to produce a stable protein. By Western blot (immunoblot) analysis of Snp1 mutant proteins in fractionated splicing extracts, we are able to confirm the stable expression of the Snp1, Δ16, mOct, mOct-ΔGly, ΔGly, and ΔC-1 proteins (data not shown). However, because of epitope loss and cross-reactive, comigrating proteins, we cannot conclusively demonstrate the stable expression of Δ59, Δ74, Δ156, and Δ169. Since three of these alleles (Δ59, Δ156, and Δ169) complement the wild type at 30°C, we are confident that all four snp1 mutant proteins are stably expressed.

A second set of mutant *snp1* alleles was targeted to the highly conserved RRM and glycine-rich domains as specific mutations, deletions, or combinations of mutations and deletions. The mOct allele substitutes 3 aa at the first, third, and fifth positions (in boldface type) of the highly conserved RNP1 octapeptide (**K**G**Y**A**F**IVF to **L**G**T**A**L**IVF). Amino acids 49 to 349 of human U1-70K, which contain the RNP1 octamer, allow efficient binding of a 70K-LacZ fusion protein to human U1 RNA in vitro (57). However, mutation of the first position in the RNP1 octamer of this fusion protein results in failure to bind U1 RNA. The co-crystal structure of a related RRM-containing protein (U1A protein-U1 RNA stem-loop II) shows multiple hydrogen bond interactions of octamer positions 3 and 5 with other RRM residues (39). Therefore, mutation of these 3 aa is predicted to disrupt U1 RNA binding and proper formation of the RRM structure. Surprisingly, the mOct allele gives full complementation at all temperatures (Fig. 3).

The ΔGly allele deletes 26 aa within the glycine-rich region that in human U1-70K protein forms part of the minimal U1 RNA binding domain (42). The mOct-ΔGly double mutant is predicted to completely ablate association of Snp1 with stem-loop I of U1 RNA. However, like the mOct allele, both ΔGly and mOct-ΔGly also complement the growth of the *snp1*-null strain, albeit less well at 37°C. These results demonstrate that the highly conserved RNP1 and glycine-rich domains are dispensable for Snp1 function.

To extend this observation, we constructed two alleles, Δ156 and Δ169, that completely remove the RRM and glycine-rich domains. Strikingly, both of these alleles allow near-wild-type growth up to 33°C (Fig. 3). The Δ156 allele complements as well as ΔGly at 37°C, demonstrating conclusively that the RRM and glycine-rich domains are not required for 70K function in vivo. The near-wild-type phenotypes of the RRM and glycine-rich domain deletion alleles correlate with the viability of the U1 RNA stem-loop I deletion strain (28). Both experiments indicate that the conventional protein-RNA interaction between the RRM domain of Snp1 and U1 RNA stem-loop I is not functionally critical.

To test if the amino-terminal domain is both necessary and sufficient for in vivo function, we constructed the Δ156-C2 mutant *snp1* allele. This allele differs from Δ156 in that it expresses only 8 carboxyl-terminal aa (aa 248 to 255) because of an engineered stop codon at aa 256. The growth phenotype and temperature sensitivity of the Δ156-C2 strain parallels those of the Δ156 strain, including slow growth at 37°C (data not shown). It is unlikely that the 8 carboxyl-terminal aa are contributing function to the Δ156-C2 protein, as these residues can be deleted without loss of function in the ΔC-1 protein. We cannot rule out the possibility, however, that these 8 aa provide a function redundant in the wild-type protein yet are critical in the Δ156 context. Among the 8 carboxyl-terminal aa are two serines and a threonine, which may be phosphorylation sites that modulate the activity of Snp1. As yet, unlike the case for human U1-70K (59, 61), we have no evidence for the regulation of Snp1 activity by phosphorylation. Taken together, these results strongly suggest that the amino-terminal domain of Snp1 is alone necessary for function.

snp1*-null strains exhibit a defect in pre-mRNA splicing.** Although *SNP1* is a nonessential gene, the *snp1*::*ADE2* gene disruption strongly perturbs growth. To determine if this growth defect is due to a reduction in pre-mRNA splicing efficiency, we analyzed pre-mRNA splicing in the YPH401- and **a**/α105-derived *snp1*-null strains. Surprisingly, primer extension analysis of efficiently spliced introns, including *ACT1* and *RPL32*, revealed that these transcripts are spliced as efficiently in the *snp1*-null strains as they are in the wild-type strains (data not shown). A pre-mRNA splicing defect in the *snp1*-null strains became apparent when we examined a number of transcripts characterized as inefficiently spliced. Primer extension analysis of the *MATa***1* transcript revealed that YPH401-derived *snp1*-null strains accumulate unspliced *MAT***a***1* precursor RNA and splicing intermediates (data not shown). Likewise, in the **a**/α105-derived *snp1*-null strains, the splicing efficiency of the *U3A* and *U3B* pre-mRNAs is reduced, as shown by the accumulation of precursor transcripts (Fig. 4, compare lanes 1 and 2). Furthermore, we note that the accumulation of the *SAR1* mature transcript is greatly reduced in these strains (see Fig. 5, lanes 1 and 2). The *SAR1* transcript contains a small intron that is very sensitive to alterations in U1 snRNP activity (22a). Accumulation of unspliced *SAR1* pre-mRNA is not concomitant with the reduced level of mature *SAR1* (data not shown). We presume that the *SAR1* pre-mRNA, if not efficiently spliced, is rapidly degraded. Thus, the reduced steady-state level of *SAR1* mRNA likely results from the failure to splice *SAR1* pre-mRNA. The reduced splicing efficiency of these three transcripts demonstrates that Snp1 is involved in pre-mRNA splicing.

The amino-terminal domain complements the *snp1*-null splicing defect. We examined each allele for the ability to complement the *snp1*-null splicing defect. Again, we assayed

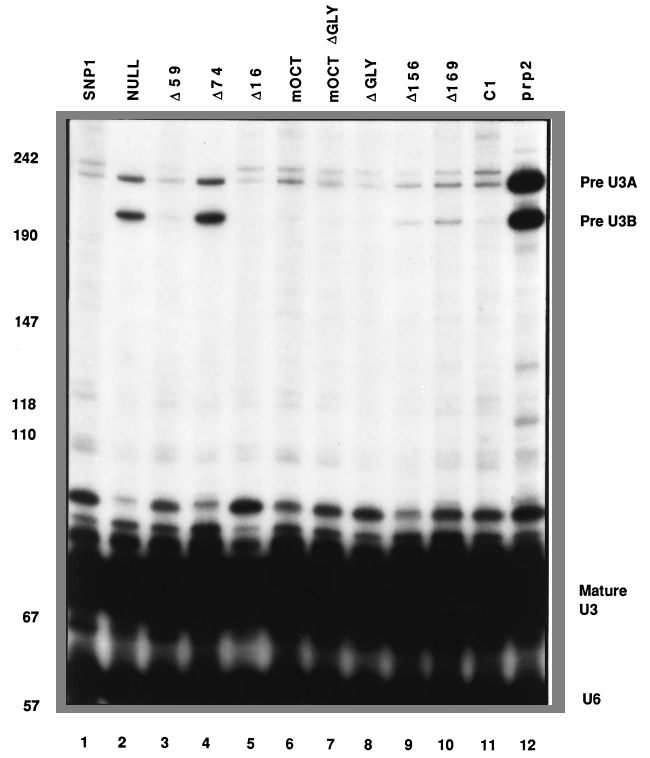

FIG. 4. U3 splicing efficiency in *snp1* mutants. 105-2A strains carrying various *snp1* alleles were grown to an A_{600} of 0.5 at 25°C and then shifted to 30°C for 6 h. RNA was harvested from each *snp1* mutant strain and analyzed by primer extension, using an oligonucleotide complementary to the pre-*U3A* and pre-*U3B* genes. RNA from a *prp2* strain shifted to 37°C is included for comparison of splicing efficiency. The positions of unspliced pre-*U3A* and pre-*U3B* precursor RNAs and of mature *U3* RNA are indicated. Also indicated is the primer extension product from a *U6* oligonucleotide included as an internal control. Shown are the primer extension products from RNA of each of the following strains: lane 1, 105-2A-*SNP1*; lane 2, 105-2A-pRS315; lane 3, 105-2A-Δ59; lane 4, 105-2A-Δ74; lane 5, 105-2A-Δ16; lane 6, 105-2A-mOct; lane 7, 105-2A-mOct-ΔGly; lane 8, 105-2A-ΔGly; lane 9, 105-2A-Δ156; lane 10, 105-2A-Δ169; lane 11, 105-2A-ΔC-1; lane 12, *prp2* shifted at 37°C for 2 h.

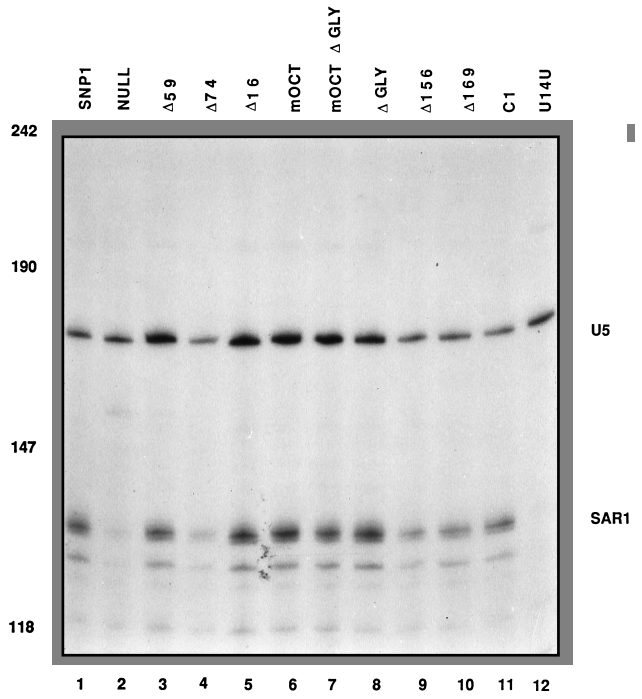

FIG. 5. Abundance of *SAR1* mature mRNA in *snp1* mutants. 105-2A strains carrying *snp1* mutant alleles were grown to an A_{600} of 0.5 at 25°C and then shifted to 30°C for 6 h. RNA was harvested from each *snp1* mutant strain and analyzed by primer extension of an oligonucleotide complementary to the *SAR1* mRNA. As a control, RNA was prepared from 105-2A strains carrying a wild-type *SNP1* gene (lane 1) or vector alone (Null, lane 2). Also, RNA was prepared from a strain carrying the *U1-4U* mutation that was shifted to 18°C for 6 h, conditions under which this cold-sensitive strain fails to splice *SAR1* transcripts (lane 12). The position of mature *SAR1* mRNA is indicated, along with that of the primer extension product from a *U5* oligonucleotide included as an internal control. Shown are the primer extension products from RNA of each of the following strains: lane 1, 105-2A-*SNP1*; lane 2, 105-2A-pRS315; lane 3, 105-2A-Δ59; lane 4, 105-2A-Δ74; lane 5, 105-2A-Δ16; lane 6, 105-2A-mOct; lane 7, 105-2A-mOct-ΔGly; lane 8, 105-2A-ΔGly; lane 9, 105-2A-Δ156; lane 10, 105-2A-Δ169; lane 11, 105-2A-ΔC-1; lane 12, strain U1-4U.

splicing of the *U3A*, *U3B*, and *SAR1* transcripts by primer extension analysis. In all cases, the ability of each allele to complement the splicing defect correlates with its complementation of the growth defect. For example, Δ74, which fails to complement the growth defect, also fails to complement the *snp1*-null splicing defect and accumulates unspliced pre-*U3A* and pre-*U3B* transcripts (Fig. 4, compare lane 4 with lane 1 [*SNP1*] and lane 2 [Null]). The alleles that complement the growth defect well, *SNP1*, Δ59, Δ16, mOct, mOct-ΔGly, ΔGly, Δ156, Δ169, and ΔC-1 (Fig. 4, lanes 1, 3, and 5 to 11, respectively) also significantly complement the splicing defect, although the Δ156 and Δ169 alleles complement less well.

Similar results were obtained by primer extension analysis of the *SAR1* transcript. In this case, splicing efficiency was measured by the accumulation of *SAR1* mRNA. *SAR1* mRNA fails to accumulate in a cold-sensitive U1 RNA mutant (Fig. 5, lane 12). Like the null strain, Δ74 accumulates little *SAR1* mature mRNA (Fig. 5, compare lane 4 with lane 1 [*SNP1*] and lane 2 [Null]), while Δ156 and Δ169 accumulate an intermediate amount of spliced product (Fig. 5, lanes 9 and 10). All other alleles show wild-type levels of the *SAR1* mature transcript (Fig. 5, lanes 1, 3, 5 to 8, and 11). These results show that the growth and temperature sensitivities observed with *snp1*-null strains correlate with a pre-mRNA splicing defect and, importantly, that the amino-terminal domain of Snp1 is necessary to complement these defects.

The amino-terminal domain associates with the U1 snRNP in vivo. Deletion of the RRM and glycine-rich domains was expected to prevent the binding of Snp1 to stem-loop I of U1 RNA. However, the fact that these alleles complement *snp1*-null strain phenotypes suggests that they can still associate with the U1 snRNP. To test if the *snp1* deletion alleles are associated with the U1 snRNP in vivo, we performed immunoprecipitations by using antisera raised against a TrpE-Snp1 fusion protein (Fig. 6). We tested their association with the U1 snRNP by assaying the immune supernatants and pellets for the presence of U1 RNA by Northern blotting. When the *snp1*-null strain carries a plasmid containing a wild-type copy of *SNP1*, 81% of the U1 RNA is detected in the immune pellet (Fig. 6, lane 2). However, in a null strain that contained the pRS315 vector, no U1 RNA is coimmunoprecipitated (Fig. 6, lane 5). Strikingly, the Δ156 allele permits coimmunoprecipitation of 23% of the U1 RNA (Fig. 6, lane 8). Similar results were obtained from coimmunoprecipitation experiments done with 50 and 350 mM NaCl (data not shown). These results indicate that the amino terminus of Snp1 is sufficient to allow in vivo association with the U1 snRNP. The Δ59, Δ16, mOct, mOct-ΔGly, ΔGly, Δ169, and ΔC-1 *snp1* alleles also allow co-

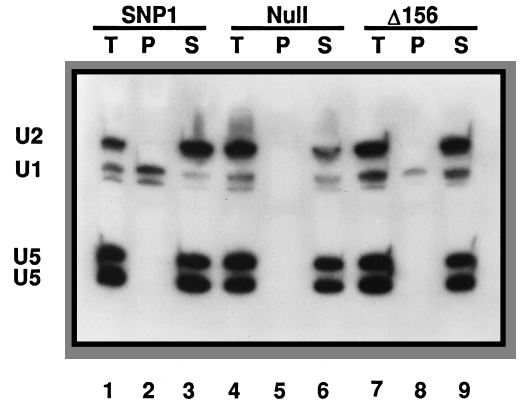

FIG. 6. Coimmunoprecipitation of U1 RNA with *snp1*-Δ156. Splicing extract was prepared from 105-2A *snp1*-null strains containing a plasmid with wild-type *SNP1* (SNP1-Leu), no *SNP1* (pRS315), or Δ156 (Δ156-Leu). Extracts were immunoprecipitated in Ipp150 (16) with affinity-purified polyclonal antisera against TrpE-Snp1. The immune supernatants and immune pellets were analyzed for the presence of spliceosomal snRNAs by Northern blotting with oligonucleotide probes specific for the U1, U2, and U5 snRNAs. For each sample, the unprecipitated total RNA (T), immune pellet RNA (P), and immune supernatant RNA (S) are shown. Lanes 1 to 3 are fractions of the 105-2A-*SNP1* splicing extracts. Lanes 4 to 6 are the fractions from the *snp1*-null strain 105-2A (transformed with the vector alone) splicing extract. Lanes 7 to 9 are the fractions of the 105-2A-Δ156 splicing extracts. Lanes 2 and 8 show specific coimmunoprecipitation of U1 RNA with the *SNP1* and Δ156 alleles. The U1 RNA yields two bands because of partial degradation. Yeast cells contain two forms of the U5 RNA.

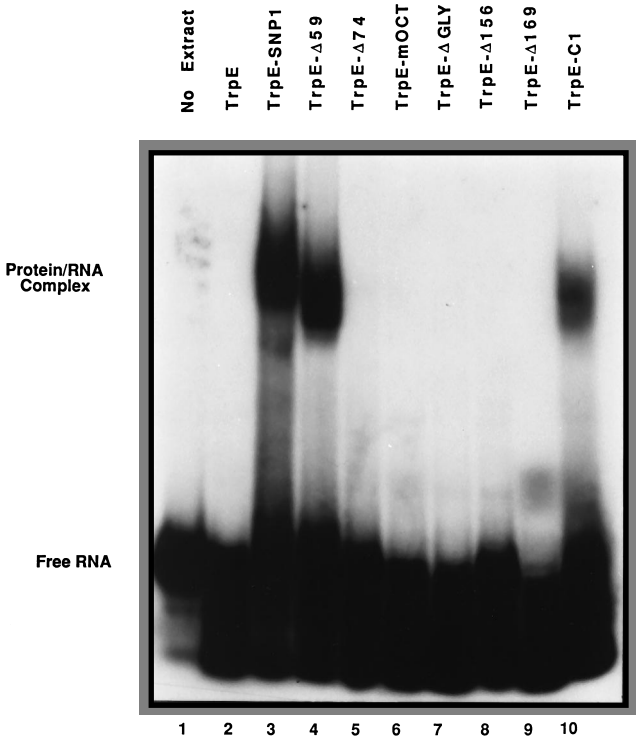

FIG. 7. In vitro binding of *snp1* mutants to U1 stem-loop I. TrpE-Snp1 fusion proteins were expressed in *E. coli* CAG456, partially purified, and incubated with a radiolabeled 47-nucleotide U1 RNA fragment encompassing stem-loop I. Complexes were resolved on a 5% native polyacrylamide gel and visualized by autoradiography. The position of the TrpE-Snp1-U1 RNA complex is indicated, as is the position of the unbound U1-stem-loop I RNA (free RNA). Lane 1, RNA alone. Lane 2, RNA incubated with extract from CAG456 transformed with the *trpE* vector, pATH3a, with no *SNP1* fusion. Specific complex formation is shown with the TrpE-SNP1, TrpE-Δ59, and TrpE-ΔC-1 extracts (lanes 3, 4, and 10, respectively). TrpE-Δ74, TrpE-mOct, TrpE-ΔGly, TrpE-Δ156, and TrpE-Δ169 (lanes 5 to 9, respectively) fail to form specific complexes with stem-loop I. The fast-migrating complex with TrpE-Δ169 (lane 9) is a nonspecific band, inconsistently seen in some extracts.

immunoprecipitation of U1 RNA (data not shown). The Δ74 allele fails to associate with the U1 snRNP, commensurately with its inability to complement the growth and splicing defects. We conclude that the RRM, glycine-rich, and carboxyl-terminal domains are not required for the association of Snp1 with the U1 snRNP. Presumably, the amino-terminal domain of Snp1 provides a second U1 snRNP interaction domain that permits stable association. These results parallel those observed with the human U1-70K protein described by Nelissen et al. (37), in which an amino-terminal fragment (aa 1 to 97) effectively associates with U1 core snRNPs.

The RRM and Gly domains are required for binding U1 RNA in vitro. To address the possibility that the amino-terminal domain binds U1 RNA directly, we tested the *snp1* deletion alleles for binding to U1 RNA in vitro. We expressed the *snp1* alleles as TrpE fusions in *Escherichia coli* and used a gel shift assay to test the binding of the TrpE-Snp1 fusion proteins to an RNA fragment encompassing stem-loop I of yeast U1 RNA (Fig. 7). We have previously shown that the binding of the TrpE-Snp1 fusion protein to the RNA fragment is specific and direct (22). The stable expression of the TrpE-Snp1 fusions was confirmed by Coomassie blue staining and Western blot analysis (data not shown). TrpE fusions of the wild-type, Δ59, and ΔC-1 proteins bind to stem-loop I of U1 RNA (Fig. 7, lanes 3, 4, and 10, respectively). However, all alleles that affect the RRM or glycine-rich domains fail to associate with the stem-loop I RNA fragment (Fig. 7, lanes 6 to 9). This result agrees with prior studies of human U1-70K that demonstrated that the RRM was essential for binding to stem-loop I in vitro (42). Interestingly, TrpE-Δ74 does not bind the stem-loop I fragment (Fig. 7, lane 5) even though this allele retains intact RRM and glycine-rich domains. It is possible that Δ74, which removes aa 19 to 92, perturbs the folding of the U1 RNA binding domain predicted by alignment to human U1-70K to begin at aa 96. This interpretation suggests that the Δ74 allele has debilitated both the amino-terminus- and the RRM-mediated U1 snRNP association domains of the Snp1 protein.

DISCUSSION

In this report we demonstrate that YPH401- and **a**/α105-derived *snp1*-null cells are viable, in contrast to the initial characterization of *SNP1* as an essential gene in the **a**/α100 strain. We also show that the Snp1 protein is involved in pre-mRNA splicing. Inefficiently spliced introns such as *MAT***a***1*, *U3A*, and *U3B* accumulate splicing precursors, and the abundance of *SAR1* mRNA is drastically reduced in *snp1*-null strains. In contrast, it is important to note that the *snp1*::*ADE2* disruption has little influence on the splicing of efficient introns such as *ACT1* (data not shown). We believe that the Snp1 protein is a constitutive splicing factor involved in the processing of all introns. Inefficiently spliced introns, whose processing is sensitive to slight perturbations in the splicing apparatus, reveal the influence of Snp1 on pre-mRNA splicing.

Unexpected features of Snp1. Analysis of domain deletion alleles of Snp1 shows several surprising and enlightening results. First, we show that the highly conserved RRM and glycine-rich domains are not required for Snp1 function in vivo. *snp1* alleles harboring mutations and deletions within these regions unexpectedly complement the *snp1*-null phenotypes up

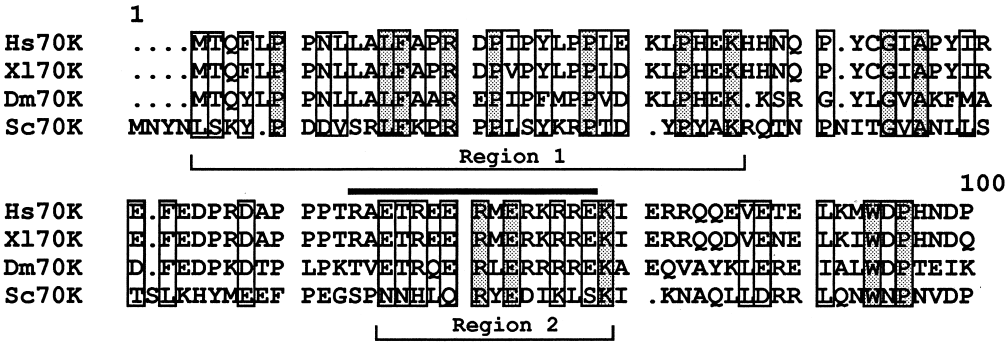

FIG. 8. Alignment of the amino-terminal residues of U1-70K proteins. Approximately 100 amino-terminal residues of human, *X. laevis*, *D. melanogaster*, and *S. cerevisiae* sequences were aligned as previously described (56). Amino acids are grouped according to the method of Taylor (58) as follows: polar nonaromatic charged (R,K,H); polar nonaromatic, nonpositive charged (T,S,N,D,E,Q); aromatic (H,W,Y,F); small hydrophobic (V,C,P,A,G); and large hydrophobic (F,M,L,I,V). Shaded boxes represent identical residues in the alignment. Open boxes represent conserved substitutions in the alignment. Highlighted by a thin bracket are the two conserved regions (1 and 2). Also indicated (by a thick bar) is the region of human U1-70K described as homologous to $p30^{gag}$ (43).

to 33°C. Furthermore, these mutant proteins efficiently associate with the U1 snRNP in vivo, as shown by the ability to coimmunoprecipitate U1 RNA when anti-TrpE-Snp1 antibodies are used. These findings now explain the near-wild-type phenotype of a stem-loop I deletion of U1 RNA (28); Snp1 can associate with the U1 snRNP without the interaction between the RRM and stem-loop I.

snp1 alleles with mutations in the RRM or glycine-rich domain expressed as TrpE fusions in *E. coli* fail to associate with stem-loop I of U1 RNA in vitro. Although other regions of the Snp1 protein could interact directly with U1 RNA, we are not able to detect other interactions in vitro. For example, the TrpE-Snp1 and TrpE-Δ59 fusion proteins efficiently coimmunoprecipitate in vitro transcribed full-length U1 RNA, but TrpE-Δ156 does not (data not shown).

The stable in vivo association of the RRM and glycine-rich domain deletion mutants within the U1 snRNP is most likely due to protein-protein contacts between Snp1 and other U1 snRNP proteins. Thus, analogous to human U1-70K, the association of Snp1 with the U1 snRNP is bipartite. The RRM binds stem-loop I of U1 RNA, and the amino terminus interacts with some other snRNP component. Strong candidates for the protein-protein interaction partner(s) of Snp1 are the Sm proteins. Human U1-70K was shown to chemically cross-link to Sm D2 and B′/B (37). Four yeast Sm core proteins have been characterized: Smd1 (47), Smd3 (45), and, recently, homologs of the metazoan F and G Sm proteins (49). It will be of interest to test if these proteins interact with Snp1.

The Snp1 protein tolerates mutations and deletions in all regions of the protein except the amino terminus. The Δ59 allele is able to complement the *snp1*-null strain fully at 30°C, yet the additional deletion of 16 carboxyl-terminal aa to yield Δ74 results in an *snp1*-null phenotype. The Δ74 allele is predicted to have an intact U1 RNA binding domain and to be able to form a stable complex with stem-loop I of U1 RNA. Interestingly, Δ74 fails to associate with the U1 RNA in vivo and in vitro. We note that the homologous minimal U1 RNA binding domain of Snp1 is predicted by alignment to human U1-70K to initiate just 4 residues downstream of the Δ74 junction, at aa 96. Therefore, it is possible that this allele has perturbed, at least locally, the structural arrangement or folding of the U1 RNA interaction domain. Thus, the Δ74 allele deletes the protein-protein interaction domain and likely perturbs the stem-loop I interaction domain, resulting in a null-like phenotype.

Snp1 was functionally characterized as the yeast U1-70K homolog on the basis of the ability of a chimeric, yeast-human protein containing the central 188 aa of human U1-70K to restore viability (56). On the basis of our observations of the dispensability of the RRM and glycine-rich domains, we believe that the complementation observed was due to a homologous functional domain provided within the amino-terminal region of human U1-70K.

Within the amino terminus of metazoan U1-70K proteins are two regions found to be highly conserved, depicted as regions 1 and 2 in Fig. 8. Among humans, *Xenopus laevis*, and *Drosophila melanogaster*, the first region of 32 aa is 100% conserved, with 75% identity. The second region, located more centrally within the amino terminus of metazoan U1-70K proteins, is 100% conserved, with 66% identity. Snp1 was not initially recognized as sharing in the strong conservation of these two amino-terminal regions. Upon further inspection, however, we believe that significant homology is maintained within these regions of the amino terminus of the yeast U1-70K protein. An alignment of the first 100 aa from *S. cerevisiae*, *X. laevis*, *D. melanogaster*, and human U1-70K proteins is shown in Fig. 8, and displays, overall, 43% conservation and 15% identity. Within the first 32 aa, the yeast sequence maintains 59% conservation and 25% amino acid identity with the metazoan U1-70K sequences. The second region is identical in this alignment at only 13% yet maintains significant conservation, at 53%. Strikingly, the second conserved region overlaps considerably the $p30^{gag}$ homology region of human U1-70K described by Query and Keene (43). Given the functional significance of the amino terminus of the human and yeast U1-70K proteins, we are intrigued at the possibility that these two regions may represent functional domains of the amino terminus.

The carboxyl terminus of Snp1 does not share the arginine-rich domains found in metazoan 70K and is completely dispensable for function (ΔC-1). The carboxyl RS domain of human U1-70K participates in a protein-protein interaction with a similar domain in SF2/ASF (24) and suggests a model for 5′ splice site recognition and association. Thus, in *S. cerevisiae*, other U1 snRNP-associated proteins may be contributing to the 5′ splice site recognition and association. A recent biochemical analysis of the yeast U1 snRNP found that it contains, in addition to the Sm core proteins, nine U1-specific proteins (14). One or more of these may be interacting specifically with Snp1 in the U1 snRNP. Identification and functional characterization of these protein-protein interactions will help

us understand the roles of snRNP proteins in pre-mRNA splicing.

ACKNOWLEDGMENTS

We thank B. Ruis for technical assistance and V. Smith and B. Barrell for plasmids and strains. In addition, we are grateful to S. Jones, J. Bodley, and M. Murphy for comments on the manuscript.

This work was supported by a grant from the NIH (GM-44628) to P.G.S.

REFERENCES

1. **Abovich, N., X. C. Liao, and M. Rosbash.** 1994. The yeast MUD2 protein: an interaction with PRP11 defines a bridge between commitment complexes and U2 snRNP addition. Genes Dev. **8:**843–854.
2. **Adam, S. A., T. Nakagawa, M. S. Swanson, T. K. Woodruff, and G. Dreyfuss.** 1986. mRNA polyadenylate-binding protein: gene isolation and sequencing and identification of a ribonucleoprotein consensus sequence. Mol. Cell. Biol. **6:**2932–2943.
3. **Bach, M., P. Bringmann, and R. Luhrmann.** 1990. Purification of small nuclear ribonucleoprotein particles with antibodies against modified nucleosides of small nuclear RNAs. Methods Enzymol. **181:**232–257.
4. **Billings, P. B., and S. O. Hoch.** 1984. Characterization of U small nuclear RNA-associated proteins. J. Biol. Chem. **259:**12850–12856.
5. **Birney, E., S. Kumar, and A. R. Krainer.** 1993. Analysis of the RNA-recognition motif and RS and RGG domains: conservation in metazoan pre-mRNA splicing factors. Nucleic Acids Res. **21:**5803–5816.
6. **Bringmann, P., and R. Luhrmann.** 1986. Purification of the individual snRNPs U1, U2, U5 and U4/U6 from HeLa cells and characterization of their protein constituents. EMBO J. **5:**3509–3516.
7. **Caceres, J. F., and A. R. Krainer.** 1993. Functional analysis of pre-mRNA splicing factor SF2/ASF structural domains. EMBO J. **12:**4715–4726.
8. **Chabot, B., D. L. Black, D. M. LeMaster, and J. A. Steitz.** 1985. The 3′ splice site of pre-messenger RNA is recognized by a small nuclear ribonucleoprotein. Science **230:**1344–1349.
9. **Cheng, S.-C., and J. Abelson.** 1987. Spliceosome assembly in yeast. Genes Dev. **1:**1014–1027.
10. **Domdey, H., B. Apostol, R.-J. Lin, A. Newman, E. Brody, and J. Abelson.** 1984. Lariat structures are in vivo intermediates in yeast pre-mRNA splicing. Cell **39:**611–621.
11. **Dreyfuss, G., M. Matunis, S. Pinol-Roma, and C. Burd.** 1993. hnRNP proteins and the biogenesis of mRNA. Annu. Rev. Biochem. **62:**289–321.
12. **Dreyfuss, G., M. S. Swanson, and S. Pinol-Roma.** 1988. Heterogeneous nuclear ribonucleoprotein particles and the pathway of mRNA formation. Trends Biochem. Sci. **13:**86–91.
13. **Etzerodt, M., R. Vignali, G. Ciliberto, D. Scherly, I. W. Mattaj, and L. Philipson.** 1988. Structure and expression of a Xenopus gene encoding an snRNP protein (U1 70K). EMBO J. **7:**4311–4321.
14. **Fabrizio, P., S. Esser, B. Kastner, and R. Luhrmann.** 1994. Isolation of S. cerevisiae snRNPs: comparison of U1 and U4/U6.U5 to their human counterparts. Science **264:**261–265.
15. **Frank, D., and C. Guthrie.** 1992. An essential splicing factor, SLU7, mediates 3′ splice site choice in yeast. Genes Dev. **6:**2112–2124.
16. **Hamm, I., M. Kazmaier, and I. Mattaj.** 1987. In vitro assembly of U1 snRNPs. EMBO J. **6:**3479–3485.
17. **Hamm, J., V. L. van Santen, R. A. Spritz, and I. W. Mattaj.** 1988. Loop I of U1 small nuclear RNA is the only essential RNA sequence for binding of specific U1 small nuclear ribonucleoprotein particle proteins. Mol. Cell. Biol. **8:**4787–4791.

17a. **Hilleren, P. J., and P. G. Siliciano.** Unpublished data.

18. **Hinterberger, M., I. Pettersson, and J. A. Steitz.** 1983. Isolation of small nuclear ribonucleoproteins containing U1, U2, U4, U5, and U6 RNAs. J. Biol. Chem. **258:**2604–2613.
19. **Ito, H., Y. Fukuda, K. Murata, and A. Kimura.** 1983. Transformation of intact yeast cells treated with alkali cations. J. Bacteriol. **153:**163–168.
20. **Jones, M., and C. Guthrie.** 1990. Unexpected flexibility in an evolutionarily conserved protein-RNA interaction: genetic analysis of the Sm binding site. EMBO J. **9:**2555–2561.
21. **Kandels-Lewis, S., and B. Seraphin.** 1993. Role of U6 snRNA in 5′ splice site selection. Science **262:**2035–2039.
22. **Kao, H.-Y., and P. G. Siliciano.** 1992. The yeast homolog of the U1 snRNP protein 70K is encoded by the SNP1 gene. Nucleic Acids Res. **20:**4009–4013.

22a. **Kao, H.-Y., and P. G. Siliciano.** Unpublished data.

23. **Koerner, T., J. Hill, A. Myers, and A. Tzagoloff.** 1991. High-expression vectors with multiple cloning sites for construction of TrpE fusion genes: pATH vectors. Methods Enzymol. **194:**477–490.
24. **Kohtz, J. D., S. F. Jamison, C. L. Will, P. Zuo, R. Luhrmann, M. A. Garcia-Bianco, and J. L. Manley.** 1994. Protein-protein interactions and 5′-splice-site recognition in mammalian mRNA precursors. Nature (London) **368:** 119–124.
25. **Kretzner, L., B. C. Rymond, and M. Rosbash.** 1987. S. cerevisiae U1 RNA is large and has limited primary sequence homology to metazoan U1 snRNA. Cell **50:**593–602.
26. **Lelay-Taha, M.-N., I. Reveillaud, J. Sri-Widada, C. Brunel, and P. Jeanteur.** 1986. RNA-protein organization of U1, U5 and U4-U6 small nuclear ribonucleoproteins in HeLa cells. J. Mol. Biol. **189:**519–532.
27. **Lesser, C. F., and C. Guthrie.** 1993. Mutational analysis of pre-mRNA splicing in Saccharomyces cerevisiae using a sensitive new reporter gene, CUP1. Genetics **133:**851–863.
28. **Liao, X., L. Kretzner, B. Seraphin, and M. Rosbash.** 1990. Universally conserved and yeast-specific U1 snRNA sequences are important but not essential for U1 snRNP function. Genes Dev. **4:**1766–1774.
29. **Lin, R.-J., A. J. Newman, S.-C. Cheng, and J. Abelson.** 1985. Yeast mRNA splicing in vitro. J. Biol. Chem. **261:**14880–14892.
30. **Luhrmann, R.** 1988. snRNP proteins, p. 71–99. *In* M. L. Birnstiel (ed.), Structure and function of major and minor small nuclear ribonucleoprotein particles. Springer-Verlag KG, Berlin.
31. **Madhani, H., and C. Guthrie.** 1992. A novel base-pairing interaction between U2 and U6 snRNAs suggests a mechanism for the catalytic activation of the spliceosome. Cell **71:**803–817.
32. **Mancebo, R., P. C. H. Lo, and S. M. Mount.** 1990. Structure and expression of the *Drosophila melanogaster* gene for the U1 small nuclear ribonucleoprotein particle 70K protein. Mol. Cell. Biol. **10:**2492–2502.
33. **Mattaj, I.** 1988. U snRNP assembly and transport, p. 100–114. *In* M. L. Birnstiel (ed.), Structure and function of major and minor small nuclear ribonucleoprotein particles. Springer-Verlag, New York.
34. **Milligan, J., and O. Uhlenbeck.** 1989. Synthesis of small RNAs using T7 RNA polymerase. Methods Enzymol. **180:**51–62.
35. **Mount, S. M., I. Pettersson, M. Hinterberger, A. Karmas, and J. A. Steitz.** 1983. The U1 small nuclear RNA-protein complex selectively binds a 5′ splice site in vitro. Cell **33:**509–518.
36. **Mount, S. M., and J. A. Steitz.** 1981. Sequence of U1 RNA from Drosophila melanogaster: implications for U1 secondary structure and possible involvement in splicing. Nucleic Acids Res. **9:**6351–6368.
37. **Nelissen, R. L. H., C. L. Will, W. J. van Venrooij, and R. Luhrmann.** 1994. The association of the U1-specific 70K and C proteins with U1 snRNPs is mediated in part by common U1 snRNP proteins. EMBO J. **13:**4113–4125.
38. **Newman, A., and C. Norman.** 1991. Mutations in yeast U5 snRNA alter the specificity of 5′ splice site cleavage. Cell **65:**115–123.
39. **Oubridge, C., N. Ito, P. Evans, C.-H. Teo, and K. Nagia.** 1994. Crystal structure at 1.92 A resolution of the RNA-binding domain of the U1A spliceosomal protein complexed with an RNA hairpin. Nature (London) **372:**432–438.
40. **Parker, R., P. G. Siliciano, and C. Guthrie.** 1987. Recognition of the TACTAAC box during mRNA splicing in yeast involves base pairing to the U2-like snRNA. Cell **49:**229–239.
41. **Pikielny, C., B. C. Rymond, and M. Rosbash.** 1986. Electrophoresis of ribonucleoproteins reveals an ordered assembly pathway of yeast splicing complexes. Nature (London) **324:**341–345.
42. **Query, C. C., R. C. Bently, and J. D. Keene.** 1989. A common RNA recognition motif identified within a defined U1 RNA binding domain of the 70K U1 snRNP protein. Cell **57:**89–101.
43. **Query, C. C., and J. D. Keene.** 1987. A human autoimmune protein associated with U1 RNA contains a region of homology that is cross-reactive with retroviral p30gag antigen. Cell **51:**211–220.
44. **Reich, C., R. VanHoy, G. Porter, and J. Wise.** 1992. Mutations at the 3′ splice site can be suppressed by compensatory base pair changes in U1 RNA in fission yeast. Cell **69:**1159–1169.
45. **Roy, J., B. Zheng, B. C. Rymond, and J. L. Woolford, Jr.** 1995. Structurally related but functionally distinct yeast Sm D core small nuclear ribonucleoprotein particle proteins. Mol. Cell. Biol. **15:**445–455.
46. **Ruby, S. W., and J. Abelson.** 1988. An early hierarchic role of U1 small nuclear ribonucleoprotein in spliceosome assembly. Science **242:**1028–1035.
47. **Rymond, B.** 1993. Convergent transcripts of the yeast PRP38-SMD1 locus encode two essential splicing factors, including the D1 core polypeptide of small nuclear ribonucleoprotein particles. Proc. Natl. Acad. Sci. USA **90:** 848–852.
48. **Sawa, H., and J. Abelson.** 1992. Evidence for a base-pairing interaction between U6 small nuclear RNA and the 5′ splice site during the splicing reaction in yeast. Proc. Natl. Acad. Sci. USA **89:**11269–11273.
49. **Seraphin, B.** 1995. Sm and Sm-like proteins belong to a large family: identification of proteins of the U6 as well as the U1, U2, U4 and U5 snRNPs. EMBO J. **14:**2089–2098.
50. **Seraphin, B., L. Kretzner, and M. Rosbash.** 1988. A U1 snRNA:pre-mRNA base pairing interaction is required early in yeast spliceosome assembly but does not uniquely define the 5′ cleavage site. EMBO J. **7:**2533–2538.
51. **Seraphin, B., and M. Rosbash.** 1989. Identification of functional U1 snRNA-pre-mRNA complexes committed to spliceosome assembly and splicing. Cell **59:**349–358.
52. **Sherman, F., G. Fink, and C. Lawrence.** 1974. Methods in yeast genetics. Cold Spring Harbor Laboratory, Cold Spring Harbor, N.Y.
53. **Siliciano, P. G., and C. Guthrie.** 1988. 5′ splice site selection in yeast: genetic

alterations in base-pairing with U1 reveal additional requirements. Genes Dev. **2:**1258–1267.
54. **Siliciano, P. G., M. Haltiner Jones, and C. Guthrie.** 1987. Saccharomyces cerevisiae has a U1-like small nuclear RNA with unexpected properties. Science **237:**1484–1487.
55. **Smith, J.** 1987. Electroelution of proteins from stained gels, p. 10.5.1–10.5.5. *In* F. Ausubel, R. Brent, R. Kingston, D. Moore, J. Smith, J. Seidman, and K. Struhl (ed.), Current protocols in molecular biology. Greene Publishing Associates, New York.
56. **Smith, V., and B. Barrell.** 1991. Cloning of a yeast U1 snRNP 70K protein homologue: functional conservation of an RNA-binding domain between yeast and humans. EMBO J. **10:**2627–2634.
57. **Surowy, C. S., V. L. van Santen, S. M. Scheib-Wixted, and R. A. Spritz.** 1989. Direct, sequence-specific binding of the human U1-70K ribonucleoprotein antigen protein to loop I of U1 small nuclear RNA. Mol. Cell. Biol. **9:**4179–4186.
58. **Taylor, W. R.** 1986. Identification of protein sequence homology by consensus template alignment. J. Mol. Biol. **188:**233–258.
59. **Tazi, J., et al.** 1993. Thiophosphorylation of U1-70K protein inhibits pre-mRNA splicing. Nature (London) **363:**283–286.
60. **Wassarman, D., and J. Steitz.** 1992. Interactions of small nuclear RNAs with precursor messenger RNA during in vitro splicing. Science **257:**1918–1925.
61. **Woppmann, A., T. Patschinsky, P. Bringmann, F. Godt, and R. Luhrmann.** 1990. Characterisation of human and murine snRNP proteins by two-dimensional gel electrophoresis and phosphopeptide analysis of U1-specific 70K protein variants. Nucleic Acids Res. **18:**4427–4438.
62. **Zamore, P. D., J. G. Patton, and M. R. Green.** 1992. Cloning and domain structure of the mammalian splicing factor U2AF. Nature (London) **355:** 609–614.
63. **Zhuang, Y., and A. M. Weiner.** 1986. A compensatory base change in U1 snRNA suppresses a 5′ splice site mutation. Cell **46:**827–835.